| | |
|---|---|
| タイトル | Full-length whole-genome sequencing analysis of emerged meropenem-resistant mutants during long- term in vitro exposure to meropenem for borderline meropenemsusceptible carbapenemase-producing and noncarbapenemase-producing Enterobacterales |
| 別タイトル | Meropenem のin vitro 長期投与で得られたmeropenem 感受性のボーダーラインであるカルバペネマーゼ産生腸内細菌目細菌と非カルバペネマーゼ産生腸内細菌目細菌由来のmeropenem 耐性株に対する全ゲノム解析 |
| 作成者（著者） | 遠藤(堤)裕子 |
| 公開者 | 東邦大学 |
| 発行日 | 2023.03.14 |
| 掲載情報 | 東邦大学大学院医学研究科 博士論文. |
| 資料種別 | 学位論文 |
| 内容記述 | 主査 : 赤羽悟美 / タイトル : Full-length whole-genome sequencing analysis of emerged meropenem-resistant mutants during long- term in vitro exposure to meropenem for borderline meropenemsusceptible carbapenemase-producing and noncarbapenemase-producing Enterobacterales /著者 : Yuko Tsutsumi Endo, Kotaro Aoki, Masakaze Hamada, Haruka Nakagawa Kamura, Yoshikazu Ishii, Kazuhiro Tateda /掲載誌 : Journal of Antimicrobial Chemotherapy /巻号・発行年等 : 78(1): 209-215, 2022 /本文ファイル: 著者版 |
| 著者版フラグ | ETD |
| 報告番号 | 32661甲第1068号 |
| 学位記番号 | 甲第740号 |
| 学位授与年月日 | 2023.03.14 |
| 学位授与機関 | 東邦大学 |
| DOI | info:doi/10.1093/jac/dkac376 |
| メタデータのＵＲＬ | https://mylibrary.toho-u.ac.jp/webopac/TD84275154 |

# Full-length whole-genome sequencing analysis of emerged meropenem-resistant mutants during long-term *in vitro* exposure to meropenem for borderline meropenem-susceptible carbapenemase-producing and non-carbapenemase-producing *Enterobacterales*

Yuko Tsutsumi Endo[a,b], Kotaro Aoki[c], Masakaze Hamada[c], Haruka Nakagawa Kamura[c], Yoshikazu Ishii[a,c*], Kazuhiro Tateda[a,c]

a Department of Microbiology and Infectious Diseases, Toho University Graduate School of Medicine, Tokyo, Japan

b Meiji Seika Pharma Co., Ltd., Tokyo, Japan

c Department of Microbiology and Infectious Diseases, Toho University School of Medicine, Tokyo, Japan

Running title: CPE analysis emerging from long-term meropenem exposure

#Address correspondence to Yoshikazu Ishii, Ph.D., Department of Microbiology and Infectious Diseases, Toho University School of Medicine, 5-21-16 Omori-nishi, Ota-ku, Tokyo 143-8540, Japan.

03-3762-4151

yishii@med.toho-u.ac.jp

Key words: carbapenemase-producing *Enterobacterales*; plasmid; whole-genome sequencing; meropenem; hollow-fibre infection model

## Abstract

**Objectives:** Molecular analysis of meropenem-resistant mechanisms in mutants emerging from long-term *in vitro* meropenem exposure to borderline meropenem-susceptible carbapenemase-producing *Enterobacterales* (CPE) and non-CPE.

**Methods:** *Escherichia coli* TUM13867 harbouring both $bla_{\text{IMP-6}}$- and $bla_{\text{CTX-M-2}}$-carrying IncN plasmid and *Citrobacter koseri* TUM13189 with $bla_{\text{CTX-M-2}}$-carrying chromosome were used. Meropenem MIC was 1 mg/L against both strains. Each strain was cultured in the hollow-fibre infection model (HFIM) to approximately $1\times10^6$ colony formation unit (cfu)/mL, and meropenem 1 g q8h treatment was initiated. Then, changes in total and meropenem-resistant populations were observed for 124 h. Meropenem resistance mechanisms were analysed by full-length whole-genome sequencing (WGS), reverse-transcription quantitative PCR, and digital PCR.

**Results:** Meropenem reduced TUM13867 and TUM13189 to approximately 5 and 2 $\log_{10}$ cfu/mL, respectively, at 2 h after initiation, but regrowth was observed at 24 h. The meropenem-resistant mutant emergence frequency at 120 h and 124 h was $4.4\times10^{-4}$ for TUM13867 and $7.6\times10^{-1}$ for TUM13189. Meropenem MIC of the mutants derived from TUM13867 (TUM20902) and TUM13189 (TUM20903) increased 4-fold and 16-fold, respectively. TUM20902, which harboured pMTY20902_IncN plasmid with a 27,505-bp deletion that included $bla_{\text{CTX-M-2}}$, and $bla_{\text{IMP-6}}$ showed 4.21-fold higher levels of transcription than the parental strain. TUM20903 had a 49,316-bp deletion that included *ompC* and a replicative increase of $bla_{\text{CTX-M-2}}$ to three copies.

**Conclusions:** Molecular analysis including complete WGS revealed that the

50 resistance mechanisms of meropenem-resistant mutants that emerged during
51 long-term *in vitro* meropenem exposure were increased $bla_{\text{IMP-6}}$ transcripts in
52 CPE and increased $bla_{\text{CTX-M-2}}$ transcripts due to gene triplication and OmpC
53 loss resulting from *ompC* deletion in non-CPE.
54

## INTRODUCTION

Effective antimicrobial treatment options for carbapenemase-producing *Enterobacterales* (CPE) infections are limited[1,2]. IMP-type (mainly IMP-1 and IMP-6) metallo-β-lactamase (MBL)-producing CPE are characteristically prevalent in Japan[3–6]. The clinical breakpoints of the Clinical and Laboratory Standards Institute (CLSI) and the European Committee on Antimicrobial Susceptibility Testing (EUCAST)[7,8] are interpreted as "susceptible" to carbapenems, carbapenems would be expected to be effective against MBL-producing bacterial infections. However, even if the interpretation was clinical susceptibility to meropenem, it has been reported that KPC-2-producing *K. pneumoniae* strains may not respond to treatment with meropenem alone[9].

In the development of novel β-lactams and β-lactamase inhibitors to support current antimicrobial agents for CPE infection, it is important to understand the mechanisms of resistance to these current antimicrobial agents. *In vitro* experiments to generate resistant bacteria are used to analyse the resistance mechanism. However, methods such as disk diffusion method, the broth microdilution method, or the chemostat model could not evaluate the emergence of resistant bacteria due to long-term antimicrobial exposure. The hollow-fibre infection model (HFIM), a non-clinical model of pharmacokinetics (PK) reproduction using a dialysis membrane module, is a system that allows antimicrobial exposure to bacteria for more than 2 weeks[10].

The mechanism of resistance of mutants that emerged during treatment in the HFIM of polymyxin B and moxifloxacin against *Escherichia coli*, ceftaroline against *Staphylococcus aureus*, and ceftazidime-avibactam

against *Pseudomonas aeruginosa* and *Mycobacterium tuberculosis* have been analysed[11–15]. In these studies, point mutations in genes were analysed mainly by whole-genome sequencing (WGS). However, to our knowledge, there are no studies of resistant bacteria that have emerged in the HFIM related to exogenous antimicrobial resistance mechanisms located on plasmids carrying the β-lactamase gene. Full-length WGS by long read sequencing, not only in parental strains but also mutant strains, can reveal dynamic structural changes around the β-lactamase gene on the plasmid due to mobile genetic elements.

Here, we evaluated meropenem-resistant mechanisms of emerged mutants by molecular methods including full-length WGS during long-term *in vitro* meropenem exposure derived from both borderline meropenem-susceptible CPE and non-CPE.

## MATERIALS AND METHODS

### Bacterial isolates

We analysed a CPE strain, *bla*$_{\text{IMP-6}}$- and *bla*$_{\text{CTX-M-2}}$-harbouring *E. coli* TUM13867, and a non-CPE strain, *bla*$_{\text{CTX-M-2}}$-harbouring *Citrobacter koseri* TUM13189, by WGS (Table 1). Meropenem MIC of both strains was 1 mg/L, indicating their susceptibility. These isolates were stored at −80°C.

### Antimicrobial susceptibility testing

Antimicrobial susceptibility testing was performed using the broth microdilution method according to the CLSI guidelines M07[16]. MIC plates treated according to the broth microdilution method were supplied by Eiken

Chemical Co., Ltd. (Tokyo, Japan). *E. coli* ATCC 25922 and *P. aeruginosa* ATCC 27853 were used as quality control strains. The MICs were interpreted according to the CLSI guidelines M100-32nd edition[7].

**Emergence frequency of meropenem-resistant mutants**

To calculate the emergence frequency of meropenem-resistant mutants, serial dilutions of the bacterial solutions in 10-fold increments were spread on Mueller–Hinton agar (MHA) (Becton, Dickinson and Company: BD, Franklin Lakes, NJ,USA) and MHA containing 3×MIC (3 mg/L) meropenem (Meiji Seika Pharma Co., Ltd., Tokyo, Japan and Fujifilm Wako Pure Chemical Corporation, Tokyo, Japan). After incubating the dishes at 35°C for 24 h, colonies grown on each MHA were counted and the emergence frequency of resistant mutants was calculated using the following equation: number of colonies on MHA containing meropenem per MHA.

**The Hollow-fibre infection model (HFIM)**

The HFIM was constructed with a central vessel (2019-0125; Thermo Fisher Scientific, Waltham, MA, USA) and a polysulphone membrane module FCS-C2011 (FiberCell Systems, New Market, MD, USA), and cation-adjusted Mueller-Hinton Broth (CAMHB, BD) was used as the culture medium. The PK parameters of meropenem based on 1-compartment PK model were calculated using Phoenix WinNonlin software (version 8.1.0, Cetera, Inc. Princeton, NJ, USA) from the concentration data of a previous report[17]. The PK parameters calculated by the WinNonlin software were as follows: Vd, 14.89 L; ke, 0.934 1/h; and CL, 13.91 L/h. Meropenem treatment (1 g, q8h, 30-min infusion) was simulated using a syringe pump (Legato 210P; KD Scientific, Holliston, MA, USA) and a peristaltic pump (MasterFlex 07522-30;

Cole-Parmer, Vernon Hills, IL, USA). A total of 20 mL tested bacterial solutions diluted in CAMHB were inoculated into the extra-capillary space (ECS) of FCS-C2011 and pre-incubated at 35°C for 3 h (to approximately $1\times10^6$ cfu/mL). After pre-incubation, meropenem infusion was initiated, and tested bacteria were incubated for 120 h or 124 h at 35°C. The conditions were set up as the non-treated control group and the meropenem-treated group (n=2). The fluid circulating through the intra-capillary space (ICS) of FCS-C2011 and the central vessel was mixed at a rate of approximately 60 mL/min using the duet pump FCS-P3202 (FiberCell Systems). Moreover, to make the bacteria in the ECS uniform, the fluid was circulated at 15 mL/min using the smooth flow pump QI-100-6TA (Tacmina, Osaka, Japan).

**Measurement of meropenem PK in the HFIM**

Meropenem PK in the HFIM was validated by running ultrapure water at room temperature. Meropenem solutions at 0.5 h and 1 h were collected from the central vessel and ECS ports, and the meropenem concentration was measured by bioassay[18]. Briefly, meropenem activity in the sample against the indicator strain, *E. coli* NIHJ JC-2, was measured by the disk diffusion method, and the meropenem concentration was calculated according to the standard curve of its inhibition zone diameter.

**Monitoring the emergence of meropenem resistance in the HFIM**

The bacterial solutions in ECS were collected from the non-treated control group and the meropenem-treated group at 0, 2, 24, 72, and 120 h or 0, 2, 24, 72, and 124 h from start of meropenem administration in the HFIM. Serial dilutions of the collected samples from the HFIM in 10-fold increments were spread onto MHA plates and MHA plates containing 3×MIC (3 mg/L)

meropenem and then cultured.

**Whole-genome sequencing analysis**

DNA was extracted using magLEAD and MagDEA Dx SV kits (Precision System Science Co., Ltd., Chiba, Japan). DNA library preparation, sequencing by MiSeq (Illumina, Inc., San Diego, CA, USA), and MinION, hybrid *de novo* assembly, gene annotation, species identification, finding acquired antimicrobial resistant genes, and detection of single nucleotide polymorphism (SNPs) were performed as previously described[19]. MAUVE was used for genome structural analysis[20].

**Conjugation experiments**

The conjugation experiments were performed as previously described[5].

**Plasmid maintenance rate and *bla*$_{\text{IMP-6}}$ transcriptional analysis**

To measure populations maintaining the *bla*$_{\text{IMP-6}}$-carrying plasmid, we developed TaqMan Probe-based digital PCR (dPCR) and quantitative PCR (qPCR). The gene encoding 1-deoxy-D-xylulose-5-phosphate synthase (*dxs*) was used as an internal control of single copy markers per cell[21]. Oligonucleotides are listed in Table S1. Total DNA and RNA were extracted from bacteria cultured in meropenem-free MHA at 35°C for 16 h by phenol-chloroform treatment and purified using the FastGene Gel/PCR Extraction Kit (Nippon Genetics Co., Ltd, Tokyo, Japan). QuantStudio 3D Digital PCR Master Mix v2 (Thermo) and QuantStudio 3D Digital PCR System (Thermo) were used for dPCR. Transcript quantification was performed by qPCR using QuantStudio 5 (Thermo) with TaqPath 1-Step RT-qPCR Master Mix (Thermo) after DNase treatment using Recombinant DNaseI (RNase-Free) (TaKaRa Bio

Inc., Siga, Japan). The *bla*$_{IMP-6}$ transcript was compared using the threshold cycle ($\Delta\Delta$Ct) method[22].

**Data availability**

WGS data of GenBank accession numbers were as follows: TUM13189, AP025640-AP025652; TUM13867, AP025657-AP025661; TUM20902, AP025662-AP025666; and TUM20903, AP025653-AP025656.

## RESULTS

### Characteristics of strains supplied to the HFIM

Two strains, CPE *E. coli* TUM13867 and non-CPE *C. koseri* TUM13189, were used to evaluate the therapeutic effect of meropenem in the HFIM (Table 1). *E. coli* TUM13867 harboured both *bla*$_{IMP-6}$ encoding IMP-6 and *bla*$_{CTX-M-2}$ encoding CTX-M-2 extended-spectrum β-lactamase (ESBL)-carrying IncN plasmid. The other, *C. koseri* TUM13189, harboured *bla*$_{CTX-M-2}$ located on its chromosome. Both strains showed MIC 1 mg/L for meropenem and were interpreted as susceptible by the CLSI clinical breakpoint. The emergence frequency of meropenem susceptibility-reduced mutants was $2.8\times10^{-4}$ for CPE TUM13867 and $2.5\times10^{-8}$ for non-CPE TUM13189.

### Validation of meropenem PK in the HFIM

Measurement values for 0.5 h and 1 h were 66.6 mg/L and 52.5 mg/L in the central vessel, 68.8 mg/L and 54.0 mg/L in the exit port of ECS, and 62.7 mg/L and 51.9 mg/L in the entrance port of ECS, respectively. Theoretical values for 0.5 h and 1 h were 53.4 mg/L and 33.5 mg/L, respectively.

**Meropenem treatment effects on CPE and non-CPE in the HFIM**

In CPE TUM13867, meropenem reduced the bacterial total population from an average of $1.1\times10^{6}$ cfu/mL to an average of $2.8\times10^{1}$ cfu/mL in the first 2 h (Figure 1). However, the total population recovered to $5.5\times10^{5}$ cfu/mL at the time of the first meropenem administration in 24 h. The total population increased to an average of $8.1\times10^{8}$ cfu/mL by 120 h after meropenem exposure. Although the meropenem-resistant population (grown on medium containing 3 mg/L meropenem) was below the limit of detection ($<10^{1}$ cfu/mL) at 24 h exposure to meropenem, these appeared at a concentration of approximately $2.7\times10^{2}$ cfu/mL at 72 h and increased to approximately $3.5\times10^{5}$ cfu/mL at 120 h (Figure 1). The meropenem-resistant mutant emergence frequency at 120 h was $4.4\times10^{-4}$ and the isolated meropenem-resistant strain (TUM20902) showed a meropenem MIC of 4 mg/L (Table 1).

In non-CPE TUM13139, meropenem reduced the bacterial total population from an average of $6.3\times10^{5}$ cfu/mL to $5.7\times10^{3}$ cfu/mL in the first 2 h and then increased to an average of $6.0\times10^{6}$ cfu/mL at 24 h of the first meropenem administration (Figure 2). The total population increased to an average of $3.1\times10^{9}$ cfu/mL by 124 h. The meropenem-resistant population appeared at an average of $1.4\times10^{2}$ cfu/mL at 24 h exposure to meropenem and increased to $3.5\times10^{5}$ cfu/mL at 72 h. At 124 h, it further increased to $2.3\times10^{9}$ cfu/mL (Figure 2). The meropenem-resistant mutant emergence frequency at 124 h was $7.6\times10^{-1}$ and the isolated meropenem-resistant strain (TUM20903) showed a meropenem MIC of 16 mg/L(Table 1). Inexplicably, meropenem-resistant populations were grown on MHA containing 3 mg/L meropenem from the meropenem non-treated control group only in the case

of non-CPE (Figure 2). However, because the two representative isolates from the meropenem susceptibility-reduced populations both showed a meropenem MIC of 2 mg/L and there was no difference in the MIC values compared with those of the parental strain, no subsequent WGS analysis was performed.

**Characterization of meropenem-resistant mechanisms**

In the meropenem-resistant mutant TUM20902 derived from CPE TUM13867, pMTY20902_IncN was found to have a 27,504-bp deletion compared with a *bla*$_{\text{IMP-6}}$- and *bla*$_{\text{CTX-M-2}}$-carrying IncN plasmid pMTY13867_IncN harboured by the parental strain (Figure 3). The deleted region contained *bla*$_{\text{CTX-M-2}}$. In addition, a 24,436-bp inversion was found in the remaining region of pMTY20902_IncN, where a repressor of IMP-6 expression encoding *ardK* had been truncated, resulting in an incomplete open reading frame (Δ*ardK*) (Figure 3). The chromosome of TUM20902 had a 234-bp deletion of the adhesin-encoding gene (locus tag: TUM13867_01110), a 30-bp deletion of a hypothetical protein-encoding gene (locus tag: TUM13867_23920), and a deletion of a non-coding region between locus tag TUM13867_34760 and TUM13867_34761, but no association with antimicrobial resistance, including meropenem, was reported.

The non-CPE meropenem-resistant mutant TUM20903 derived from TUM13139 harboured triplicate *bla*$_{\text{CTX-M-2}}$, while TUM13139 harboured a single copy (Figure 4). TUM20903 had 35,313-bp insertion upstream of the "IS*Ecp1*-*bla*$_{\text{CTX-M-2}}$" element. The insertion unit comprised 14 genes starting from IS*Ecp1*, and finally, three of the insertion units were tandem on TUM20903 (Figure 4). Furthermore, TUM20903 chromosome had a 49,316-

bp deletion (Figure 4). The deleted region contained the outer membrane protein C (OmpC) family encoding *ompC* (Table S2).

**Characterization of *bla*$_{IMP-6}$-carrying plasmid and *bla*$_{IMP-6}$ transcript**

Both pMTY13867_IncN and pMTY20902_IncN were conjugally transferred to *E. coli*. These transconjugants were named TUM20904 and TUM20905, respectively (Table 1). Both meropenem MICs for transconjugants were increased by 33-fold or more, but the imipenem MIC did not increase 2-fold or more compared with that of the recipient strain. Ceftazidime, ceftolozane/tazobactam, and latamoxef MIC for TUM20905 were 4-fold higher than TUM20904.

The maintained pMTY20902_IncN frequency in TUM20902 was on average 4.18-fold higher than the pMTY13867_IncN parental plasmid maintained in TUM13867 by dPCR (Figure 5A). In correlation, the amount of *bla*$_{IMP-6}$ transcript in TUM20902 was on average 4.21-fold higher than in TUM13867 (Figure 5B). Interestingly, while the maintained plasmid frequency in the transconjugant TUM20904 was on average 4.90-fold higher than the transconjugant TUM20905 (Figure 5A), both *bla*$_{IMP-6}$ transcript levels were approximately the same (Figure 5B).

## DISCUSSION

We evaluated the meropenem-resistant mechanisms of mutants that emerged during long-term *in vitro* meropenem exposure derived from borderline meropenem-susceptible CPE and non-CPE. In both types of organisms, we observed what appeared to be treatment failure with

meropenem and the emergence of meropenem-resistant mutants.

The *bla*$_{IMP-6}$ transcript level in meropenem-resistant mutant TUM20902 was increased compared with that in TUM13867, suggesting that high IMP-6 expression resulted in increased MIC values for meropenem. The increased transcription of *bla*$_{IMP-6}$ in TUM20902 may be due to truncation of *ardK*[23] as well as increases in the maintained plasmid frequency per population or increased *bla*$_{IMP-6}$-carrying plasmid copy number per cell. Unfortunately, dPCR in extracted DNA cannot distinguish between the maintained plasmid frequency per cell and the plasmid copy number per cell. Interestingly, the transconjugant TUM20905 showed a distinctly lower maintained plasmid frequency, contrary to the donor strain. We hypothesized with reference to previous reports that the high IMP-6 MBL expression from *bla*$_{IMP-6}$ on pMTY20902_IncN may be toxic to the host strain[24]. The MBL accumulated in the bacteria are encapsulated in the outer-membrane vesicles and released outside the bacteria[25], but laboratory strains used as recipients in the conjugation experiments may have a lower detoxification capacity than the clinically isolated strain TUM13867. However, there were no differences in meropenem MIC values between TUM20904 and TUM20905 because *bla*$_{IMP-6}$ transcript in bulk was almost equal.

The meropenem resistance mechanisms of the non-CPE-derived meropenem-resistant mutant TUM20903 are most likely CTX-M-2 mass expression due to triplicated *bla*$_{CTX-M-2}$ and loss of the OmpC family porin due to deletion of *ompC* on the chromosome. In addition, high expression of chromosomal AmpC in *C. koseri* may contribute to meropenem resistance[26,27]. In Gram-negative bacteria, it has been reported that

meropenem or imipenem loading resulted in the emergence of resistant mutants in which large genomic changes or deletion of 479 kb of chromosome occurred[28,29]. It is likely that Gram-negative mutant strains that developed dynamic genomic variations in response to antimicrobial load at the mutant selection window were selected and adapted to the environment[30].

This study had multiple limitations. First, it should be noted the CPE and non-CPE applied in the HFIM were of a different species and background, including the presence or absence of chromosomal AmpC. WGS data did not detect any mutations that could increase AmpC production in the mutant strain, and thus AmpC production changes were not evaluated[31]. Second, IMP-6 protein expression was not measured. Third, the main carbapenem resistance mechanism of non-CPE was speculated to be a genetic deletion of *ompC*, but a complementation experiment was not performed. Fourth, β-lactamase (approximately 40 kDa), which is larger than the molecular weight cut off (20 kDa) of the HFIM membrane module FCS-C2011 used in this study, may accumulate in the ECS and reduce meropenem activity[32]. Fifth, in infectious disease treatment, antimicrobials assist host immunity, and the HFIM does not consider immunity. However, the HFIM is significant in that it provides a workflow to confirm a meropenem dosing design in which no resistance mutants appear, and then to validate the usefulness of the dosing design in future clinical trials. Sixth, We used bioassay as our method for measuring meropenem concentrations. For more accurate measurement of antimicrobial concentrations, mass spectrometry such as LC-MS should be used, but we had difficulty accessing it.

This study demonstrated that the mechanisms of meropenem

resistance in mutants that emerged during long-term *in vitro* meropenem exposure to borderline meropenem-susceptible organisms were increased *bla*$_{IMP-6}$ transcripts associated with deletion of half of the IncN plasmid sequence in CPE, and increased *bla*$_{CTX-M-2}$ transcripts due to gene triplication and OmpC loss resulting from *ompC* deletion in non-CPE.

**Funding**

This work was supported by the JSPS KAKENHI Grant-in-Aid for Scientific Research(C) to YI [grant number JP18K08452].

**Conflict of interest**

YE is an employee of Meiji Seika Pharma Co., Ltd. All other authors have no conflicts of interest to declare.

**ACKNOWLEDGMENTS**

We thank to Mr. Takuto Terada, Mr. Kohji Komori, and Mr. Shota Miura of our laboratory for their help with the experiments. We also thank H. Nikki March, PhD, from Edanz (https://jp.edanz.com/ac) for editing a draft of this manuscript.

## REFERENCES


1. Rodríguez-Baño J, Gutiérrez-Gutiérrez B, Machuca I, *et al.* Treatment of Infections Caused by Extended-Spectrum-Beta-Lactamase-, AmpC-, and Carbapenemase-Producing Enterobacteriaceae. *Clin Microbiol Rev* 2018; **3**(2): e00079-17.

2. Bush K, Bradford PA. Epidemiology of β-Lactamase-Producing Pathogens. *Clin Microbiol Rev* 2020; **33**: e00047-19.

3. Logan LK, Weinstein RA. The Epidemiology of Carbapenem-Resistant Enterobacteriaceae: The Impact and Evolution of a Global Menace. *J Infect Dis* 2017; **215**: S28–36.

4. Yonekawa S, Mizuno T, Nakano R, *et al.* Molecular and Epidemiological Characteristics of Carbapenemase-Producing *Klebsiella pneumoniae* Clinical Isolates in Japan. *mSphere* 2020; **5**: e00490-20.

5. Aoki K, Harada S, Yahara K, *et al.* Molecular Characterization of IMP-1-Producing *Enterobacter cloacae* Complex Isolates in Tokyo. *Antimicrob Agents Chemother* 2018; **62**: 02091–02017.

6. Shigemoto N, Kuwahara R, Kayama S, *et al.* Emergence in Japan of an imipenem-susceptible, meropenem-resistant *Klebsiella pneumoniae* carrying *bla*$_{\text{IMP-6}}$. *Diagn Microbiol Infect Dis* 2012; **72**: 109–12.

7. CLSI. Performance standards for antimicrobial susceptibility testing—32nd edition: M100. 2022.

8. The European Committee on Antimicrobial Susceptibility Testing. Breakpoint tables for interpretation of MICs and zone diameters, bacteria version 12.0. *EUCAST* 2022. *available at* https://www.eucast.org/fileadmin/src/media/PDFs/EUCAST_files/Breakpoint_tables/v_12.0_Breakpoint_Tables.pdf

9. Gagetti P, Pasteran F, Martinez MP, *et al.* Modeling meropenem treatment, alone and in combination with daptomycin, for KPC-producing *Klebsiella pneumoniae* strains with unusually low carbapenem MICs. *Antimicrob Agents Chemother* 2016; **60**: 5047–50.

10. Sadouki Z, McHugh TD, Aarnoutse R, *et al.* Application of the hollow fibre infection model (HFIM) in antimicrobial development: a systematic review and recommendations of reporting. *J Antimicrob Chemother* 2021; **76**: 2252–9.

11. Singh R, Ledesma KR, Chang K-T, *et al.* Pharmacodynamics of moxifloxacin against a high inoculum of *Escherichia coli* in an in vitro infection model. *J Antimicrob Chemother* 2009; **64**: 556–62.

12. Bulman ZP, Chen L, Walsh TJ, *et al.* Polymyxin Combinations Combat *Escherichia coli* Harboring *mcr-1* and *bla*$_{\text{NDM-5}}$: Preparation for a Postantibiotic Era. *MBio* 2017; **8**: e00540-17.

13. Singh R, Almutairi M, Alm RA, *et al.* Ceftaroline efficacy against high-MIC clinical

*Staphylococcus aureus* isolates in an in vitro hollow-fibre infection model. *J Antimicrob Chemother* 2017; **72**: 2796–803.

14. Drusano GL, Bonomo RA, Marshall SM. Emergence of Resistance to Ceftazidime-Avibactam in a *Pseudomonas aeruginosa* Isolate Producing Derepressed *bla*$_{PDC}$ in a Hollow-Fiber Infection Model. *Antimicrob Agents Chemother* 2021; **65**: e00124-21.

15. Deshpande D, Srivastava S, Chapagain M, *et al.* Ceftazidime-avibactam has potent sterilizing activity against highly drug-resistant tuberculosis. *Sci Adv* 2017; **3**: e1701102.

16. CLSI. Methods for dilution antimicrobial susceptibility tests for bacteria that grow aerobically—11th Edition: M07. 2018.

17. Saito A. Pharmacokinetic Study on Meropenem. *Chemotherapy* 1992; **40**: 276–82.

18. Teiji Tomio, Hiroshi Nouda, Tsuneo Kohzuki, *et al.* Assay of Meropenem in Body Fluids and Tissues. *Chemotherapy* **40**: 114–22.

19. Sugita K, Aoki K, Komori K, *et al.* Molecular Analysis of *bla*$_{KPC-2}$-Harboring Plasmids: Tn*4401a* Interplasmid Transposition and Tn*4401a*-Carrying ColRNAI Plasmid Mobilization from *Klebsiella pneumoniae* to *Citrobacter europaeus* and *Morganella morganii* in a Single Patient. *mSphere* 2021; **6**: e0085021.

20. Darling ACE, Mau B, Blattner FR, *et al.* Mauve: multiple alignment of conserved genomic sequence with rearrangements. *Genome Res* 2004; **14**: 1394–403.

21. Lee C, Kim J, Shin SG, *et al.* Absolute and relative QPCR quantification of plasmid copy number in *Escherichia coli*. *J Biotechnol* 2006; **123**: 273–80.

22. Jozefczuk J, Adjaye J. Quantitative real-time PCR-based analysis of gene expression. *Methods Enzymol* 2011; **500**: 99–109.

23. Segawa T, Sekizuka T, Suzuki S, *et al.* The plasmid-encoded transcription factor ArdK contributes to the repression of the IMP-6 metallo-β-lactamase gene *bla*$_{IMP-6}$, leading to a carbapenem-susceptible phenotype in the *bla*$_{IMP-6}$-positive *Escherichia coli* strain A56-1S. *PLoS One* 2018; **13**: e0208976.

24. Cheung CHP, Alorabi M, Hamilton F, *et al.* Trade-offs between antibacterial resistance and fitness cost in the production of metallo-β-lactamases by Enteric bacteria manifest as sporadic emergence of carbapenem resistance in a clinical setting. *Antimicrob Agents Chemother* 2021; **65**: e0241220.

25. González LJ, Bahr G, Nakashige TG, *et al.* Membrane anchoring stabilizes and favors secretion of New Delhi metallo-β-lactamase. *Nat Chem Biol* 2016; **12**: 516–22.

26. Majewski P, Wieczorek P, Ojdana D, *et al.* Altered Outer Membrane Transcriptome Balance with AmpC Overexpression in Carbapenem-Resistant *Enterobacter cloacae*. *Front Microbiol* 2016; **7**: 2054.

27. Flury BB, Ellington MJ, Hopkins KL, *et al.* Association of Novel Nonsynonymous Single Nucleotide Polymorphisms in *ampD* with Cephalosporin Resistance and

Phylogenetic Variations in *ampC*, *ampR*, *ompF*, and *ompC* in *Enterobacter cloacae* Isolates That Are Highly Resistant to Carbapenems. *Antimicrob Agents Chemother* 2016; **60**: 2383–90.

28. Fluit AC, Rentenaar RJ, Ekkelenkamp MB, *et al.* Fatal Carbapenem Resistance Development in *Pseudomonas Aeruginosa* Under Meropenem Monotherapy, Caused by Mutations in the OprD Outer Membrane Porin. *Pediatr Infect Dis J* 2019; **38**: 398–9.

29. Wardell SJT, Rehman A, Martin LW, *et al.* A large-scale whole-genome comparison shows that experimental evolution in response to antibiotics predicts changes in naturally evolved clinical *Pseudomonas aeruginosa*. *Antimicrob Agents Chemother* 2019; **63**: e01619-19.

30. Li J, Xie S, Ahmed S, *et al.* Antimicrobial Activity and Resistance: Influencing Factors. *Front Pharmacol* 2017; **8**: 364.

31. Tamma PD, Doi Y, Bonomo RA, *et al.* A Primer on AmpC β-Lactamases: Necessary Knowledge for an Increasingly Multidrug-resistant World. *Clin Infect Dis* 2019; **69**: 1446–55.

32. Bulitta JB, Hope WW, Eakin AE, *et al.* Generating Robust and Informative Nonclinical In Vitro and In Vivo Bacterial Infection Model Efficacy Data To Support Translation to Humans. *Antimicrob Agents Chemother* 2019; **63**: e02307-18.

## Table 1. Susceptibility testing of antimicrobial agents against tested strains

| Strain ID | TUM13867 | TUM13189 | TUM20902 | TUM20903 | TUM20904 | TUM20905 | TUM2236 (ML4909) |
|---|---|---|---|---|---|---|---|
| Species | *Escherichia coli* | *Citrobacter koseri* | *Escherichia coli* | *Citrobacter koseri* | *Escherichia coli* | *Escherichia coli* | *Escherichia coli* |
| Source | Original | Original | Derived from TUM13867 | Derived from TUM13189 | Transconjugant of pMTY13867_IncN plasmid from TUM13867 | Transconjugant of pMTY20902_IncN plasmid from TUM20902 | Recipient |
| Category | CPE | Non-CPE | CPE | Non-CPE | CPE | CPE | Non-CPE |
| Acquired β-lactamase genes | *bla*$_{IMP-6}$, *bla*$_{CTX-M-2}$ (on IncN) | *bla*$_{CTX-M-2}$ (on chromosome) | *bla*$_{IMP-6}$ (on IncN) | *bla*$_{CTX-M-2}$ (on chromosome) | *bla*$_{IMP-6}$, *bla*$_{CTX-M-2}$ (on IncN) | *bla*$_{IMP-6}$ (on IncN) | None |
| MIC (mg/L) | | | | | | | |
| Cefotaxime | 128 | >128 | 32 | >128 | 64 | 32 | ≤0.06 |
| Ceftazidime | 4 | >128 | 32 | >128 | 4 | 16 | 0.12 |
| Ceftolozane/tazobactam [a)] | 4 | 128 | 16 | >128 | 2 | 8 | 0.12 |
| Latamoxef | 64 | 64 | >128 | >128 | 32 | 128 | 0.12 |
| Aztreonam | 4 | >128 | ≤0.06 | >128 | 1 | ≤0.06 | ≤0.06 |
| Meropenem | 1 | 1 | 4 | 16 | 2 | 2 | ≤0.06 |
| Imipenem | 0.12 | 0.5 | 0.12 | 8 | 0.5 | 0.5 | 0.25 |
| Imipenem/relebactam [a)] | 0.12 | 0.5 | 0.12 | 4 | 0.5 | 0.5 | 0.25 |

a) Tazobactam and relebactam were a fixed concentration of 4 mg/L.

CPE, carbapenemase-producing Enterobacteriaceae

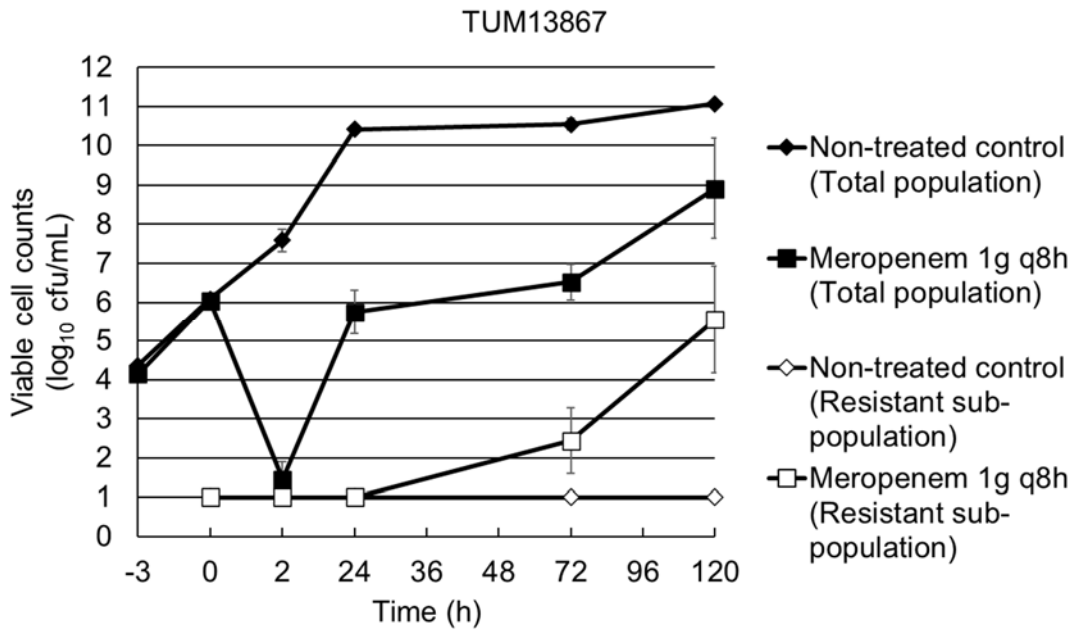


**Figure 1. Results of the hollow-fibre infection model for *E. coli* TUM13867 of total population and meropenem-resistant sub-populations exposed to meropenem 1 g q8h compared with the results of non-treated controls.**

Total population, colonies grown on MHA; resistant sub-population, colonies grown on MHA containing 3 mg/L meropenem. The limit of detection was 1 $\log_{10}$ cfu/mL. Hollow-fibre infection model experiments were performed in duplicate, and the data are presented as the means±standard deviations.

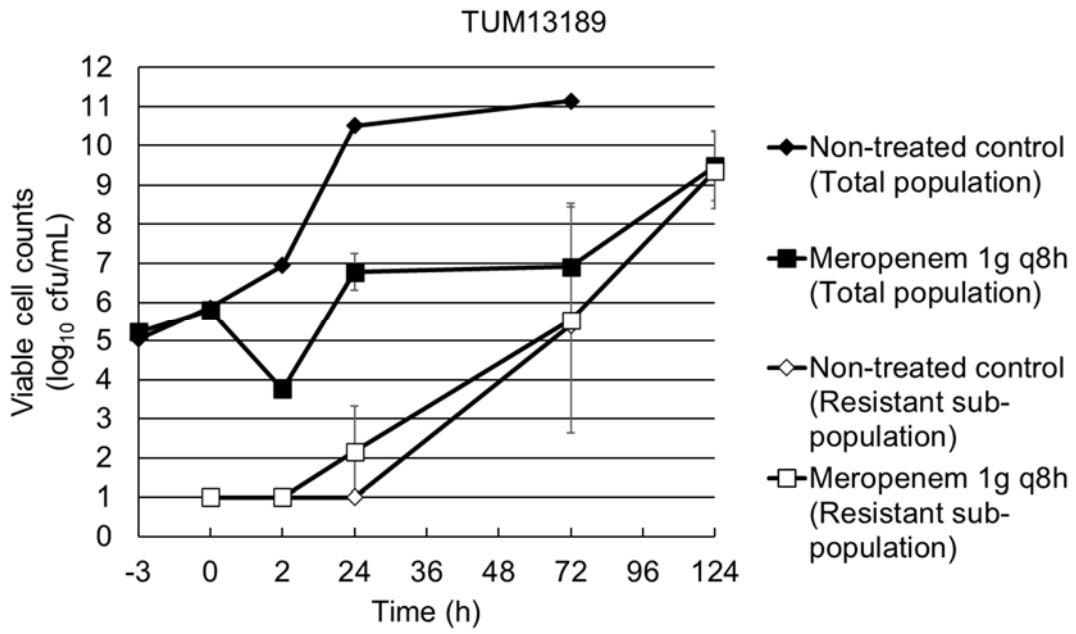


**Figure 2. Results of the hollow-fibre infection model for *C. koseri* TUM13189 of total population and meropenem-resistant sub-populations exposed to meropenem 1 g q8h compared with the results of non-treated controls.**

Total population, colonies grown on MHA; resistant sub-population, colonies grown on MHA containing 3 mg/L meropenem. The limit of detection was 1 $\log_{10}$ cfu/mL. Hollow-fibre infection model experiments were performed in duplicate, and the data are presented as the means±standard deviations.

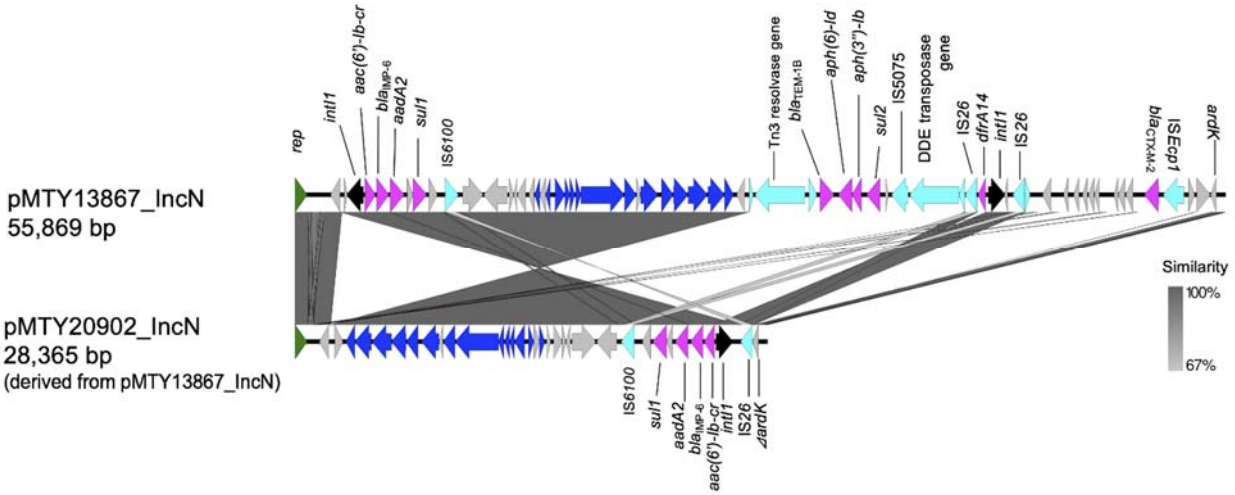


**Figure 3. Comparison of *bla*$_{IMP-6}$-carrying_IncN plasmid.**

pMTY13867_IncN harbours both *bla*$_{IMP-6}$- and *bla*$_{CTX-M-2}$-carrying plasmid in TUM13867. pMTY20902_IncN harbours *bla*$_{IMP-6}$-carrying plasmid in TUM20902, a meropenem-resistant mutant strain derived from TUM13867. pMTY20902_IncN had a 27,504-bp deletion, which included *bla*$_{CTX-M-2}$, compared with pMTY13867_IncN. The deletion or inversion disrupted *ardK* on pMTY20902_IncN. Block arrows indicate confirmed or putative open reading frames (ORFs) and their orientations. Arrow size was proportional to the predicted ORF length. The colour code was as follows: green, replication initiation protein genes; blue, conjugal transfer genes; cyan, transposase genes; black, integrase genes; magenta, antibiotic resistance genes; putative, hypothetical, and unknown genes represented by white arrows.

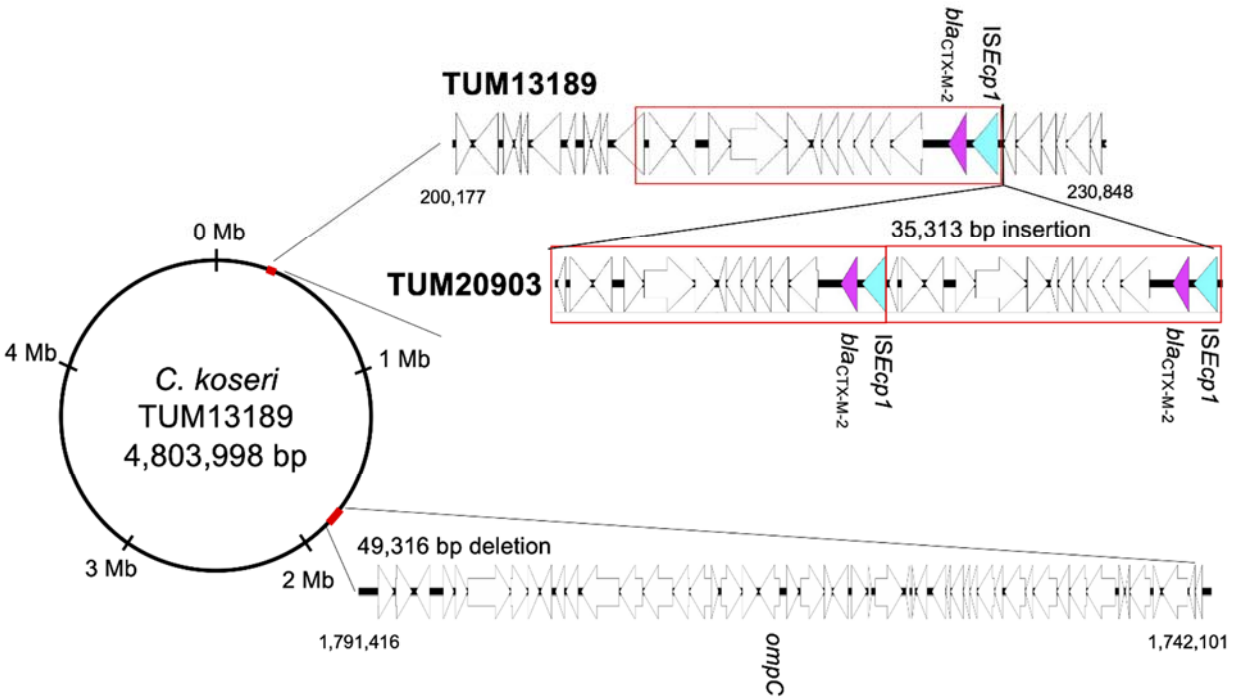


**Figure 4. A large insertion and a deletion detected in the chromosome of the meropenem-resistant mutant TUM20903 derived from TUM13189.**

Red boxes show identical nucleotide sequence units. The units may be mediated by IS*Ecp1*. Two units were inserted into the TUM20903 chromosome position upstream of IS*Ecp1*-*bla*$_{\text{CTX-M-2}}$. In addition, TUM20903 had a 49,316-bp deletion that included *ompC*.

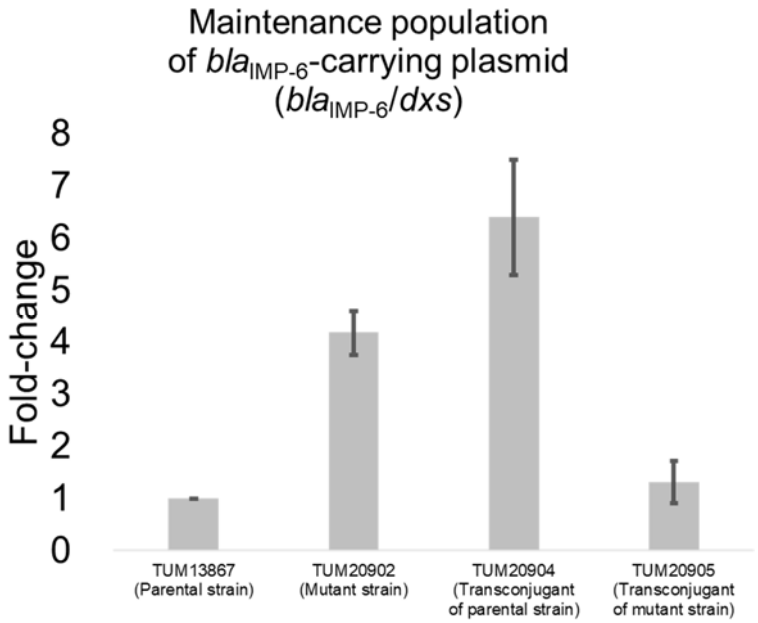


**A**

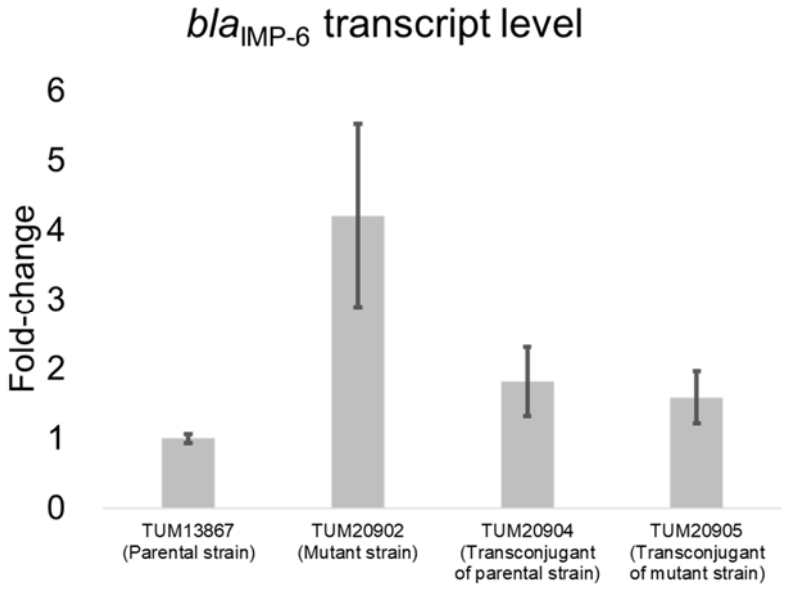


**B**

**Figure 5. Maintenance population of *bla*$_{IMP-6}$-carrying plasmids and *bla*$_{IMP-6}$ transcript level.**

A, Fold-changes in the maintenance population of *bla*$_{IMP-6}$-carrying plasmids were calculated by DNA copy number of *bla*$_{IMP-6}$ per *dxs* based on digital PCR (dPCR) data. B, Fold-changes in the *bla*$_{IMP-6}$ transcript were calculated by transcript copy number of

*bla*$_{IMP-6}$ measured by quantitative PCR normalized by DNA copy number of *dxs* based on dPCR. Error bars indicate standard deviation. The basis for the ratio calculation was TUM13867.

Table S1. Primers and probes for dPCR and qPCR

| Primer name | Sequence (5'- -3') | Final concentration for dPCR | Final concentration for qPCR |
|---|---|---|---|
| *bla*$_{IMP}$_Fw | AGACGGTAAGGTTCAAGCCA | 200 nM | 200 nM |
| *bla*$_{IMP}$_Rv | GCGTCACCCAAATTGCCTAA | 200 nM | 200 nM |
| *bla*$_{IMP}$_Probe | FAM- AACGTAGTGGTTTGGTTGCC -MGB | 100 nM | 200 nM |
| *dxs*_Fw | ACACCCCGTTTGACCAATTG | 200 nM | 200 nM |
| *dxs*_Rv | GAGGTTGATGAATGCCCGAC | 200 nM | 200 nM |
| *dxs*_Probe | VIC- ATGTGGGGCATCAGGCTTAT -MGB | 100 nM | 100 nM |

Primers and probes were constructed by primer3 web tool (https://bioinfo.ut.ee/primer3-0.4.0/). MGB, minor groove binder.

Table S2. Gene annotation information for the chromosomal deletion region in TUM20903

| Locus ID | Start | End | Strand | Gene name | Gene product (DFAST) |
|---|---|---|---|---|---|
| TUM13189_16360 | 1741716 | 1742726 | + | NA | ABC transporter permease |
| TUM13189_16370 | 1743228 | 1744145 | + | NA | LysR family transcriptional regulator |
| TUM13189_16380 | 1744247 | 1745197 | + | *cbl* | HTH-type transcriptional regulator cbl |
| TUM13189_16390 | 1745411 | 1746208 | − | *mtfA* | Protein MtfA |
| TUM13189_16400 | 1747001 | 1747609 | + | NA | Fimbrial protein |
| TUM13189_16410 | 1747705 | 1748406 | + | NA | Pilus assembly protein |
| TUM13189_16420 | 1748418 | 1750904 | + | *mrkC* | Outer membrane usher protein |
| TUM13189_16430 | 1750895 | 1751890 | + | NA | Fimbrial protein |
| TUM13189_16440 | 1751905 | 1752555 | + | NA | Hypothetical protein |
| TUM13189_16450 | 1752615 | 1753259 | − | NA | Diguanylate phosphodiesterase |
| TUM13189_16460 | 1753474 | 1753998 | − | NA | Helix-turn-helix transcriptional regulator |
| TUM13189_16470 | 1754074 | 1754787 | − | NA | Pilus assembly protein PilZ |
| TUM13189_16480 | 1754964 | 1757162 | − | *iutA* | Ligand-gated channel protein |
| TUM13189_16490 | 1757191 | 1758525 | − | NA | Lysine 6-monooxygenase |
| TUM13189_16500 | 1758529 | 1760262 | − | *iucC* | Aerobactin synthase IucC |
| TUM13189_16510 | 1760262 | 1761209 | − | *iucB* | N(6)-hydroxylysine O-acetyltransferase |
| TUM13189_16520 | 1761210 | 1762607 | − | *iucA* | Aerobactin synthase IucA |
| TUM13189_16530 | 1762494 | 1762913 | + | NA | Hypothetical protein |
| TUM13189_16540 | 1763067 | 1764278 | + | *shiF* | MFS transporter |
| TUM13189_16550 | 1764294 | 1765190 | + | NA | Siderophore-interacting protein |
| TUM13189_16560 | 1765255 | 1766436 | − | *ompC* | Outer membrane protein OmpC |
| TUM13189_16570 | 1766845 | 1767540 | + | NA | Phosphohydrolase |
| TUM13189_16580 | 1767652 | 1769046 | + | *dcm* | Cytosine-specific methyltransferase |
| TUM13189_16590 | 1769027 | 1769497 | + | NA | Very short patch repair endonuclease |
| TUM13189_16600 | 1769486 | 1770406 | − | NA | Drug/metabolite exporter YedA |
| TUM13189_16610 | 1770599 | 1771495 | + | *yedI* | Membrane protein |
| TUM13189_16620 | 1771574 | 1771756 | + | NA | Hypothetical protein |
| TUM13189_16630 | 1771969 | 1773570 | + | *yedQ* | Cellulose synthesis regulatory protein |
| TUM13189_16640 | 1773741 | 1773968 | − | *yodD* | Hypothetical protein |
| TUM13189_16650 | 1774099 | 1774287 | + | *dsrB* | Protein DsrB |
| TUM13189_16660 | 1774343 | 1774966 | − | *rcsA* | Transcriptional regulatory protein RcsA |
| TUM13189_16670 | 1775247 | 1776041 | − | *fliR* | Flagellar biosynthetic protein FliR |
| TUM13189_16680 | 1776048 | 1776317 | − | *fliQ* | Flagellar biosynthetic protein FliF |

| | | | | | |
|---|---|---|---|---|---|
| TUM13189_16690 | 1776327 | 1777064 | − | *fliP* | Flagellar biosynthetic protein FliP |
| TUM13189_16700 | 1777064 | 1777438 | − | *fliO* | Flagellar protein |
| TUM13189_16710 | 1777441 | 1777854 | − | *fliN* | Flagellar motor switch protein FliN |
| TUM13189_16720 | 1777851 | 1778855 | − | *fliM* | Flagellar motor switch protein FliM |
| TUM13189_16730 | 1778860 | 1779327 | − | NA | Flagellar basal body-associated protein FliL |
| TUM13189_16740 | 1779432 | 1780646 | − | NA | Flagellar hook-length control protein |
| TUM13189_16750 | 1780643 | 1781086 | − | *fliJ* | Flagellar FliJ protein |
| TUM13189_16760 | 1781108 | 1782478 | − | *fliI* | Flagellum-specific ATP synthase |
| TUM13189_16770 | 1782478 | 1783182 | − | NA | Flagellar assembly protein FliH |
| TUM13189_16780 | 1783175 | 1784173 | − | *fliG* | Flagellar motor switch protein FliG |
| TUM13189_16790 | 1784163 | 1785839 | − | NA | Flagellar M-ring protein |
| TUM13189_16800 | 1786056 | 1786370 | + | *fliE* | Flagellar hook-basal body complex protein FliE |
| TUM13189_16810 | 1786434 | 1786667 | − | *yedF* | UPF0033 protein YedF |
| TUM13189_16820 | 1786664 | 1787869 | − | NA | Hypothetical protein |
| TUM13189_16830 | 1788056 | 1788469 | + | NA | Lipoprotein |
| TUM13189_16840 | 1788551 | 1790038 | − | *amyA* | Cytoplasmic alpha-amylase |
| TUM13189_16850 | 1790106 | 1790468 | − | *fliT* | Flagellar protein FliT |
| TUM13189_16860 | 1790468 | 1790878 | − | *fliS* | Flagellar protein FliS |
| TUM13189_16870 | 1790888 | 1792315 | − | *fliD* | Flagellar hook-associated protein 2 |

Genes deleted in TUM20903 are indicated using the locus ID of the parental strain TUM13189. The gene locus IDs TUM13189_16360 and TUM13189_16870 at both ends of the deletion have partial open reading frames remaining on the chromosome TUM20903.